Materials Science and Engineering B 167 (2010) 55–59

Contents lists available at ScienceDirect

Materials Science and Engineering B

journal homepage: www.elsevier.com/locate/mseb

Characterization of TiO_2–Al_2O_3 composite fibers formed by electrospinning a sol–gel and polymer mixture

A.F. Lotus[a], R.K. Feaver[b], L.A. Britton[c], E.T. Bender[d], D.A. Perhay[b], N. Stojilovic[e], R.D. Ramsier[c,f,g], G.G. Chase[a,*]

[a] Department of Chemical and Biomolecular Engineering, The University of Akron, 185 E Mill Street, Akron, OH 44325, USA
[b] Physics Department, John Carroll University, University Heights, OH 44118, USA
[c] Department of Chemistry, The University of Akron, Akron, OH 44325, USA
[d] Department of Medical Physics, The University of Wisconsin-Madison, Madison, WI 53705, USA
[e] Department of Physics and Astronomy, University of Wisconsin Oshkosh, Oshkosh, WI 54901, USA
[f] Department of Physics, The University of Akron, Akron, OH 44325, USA
[g] Office of the Provost, The University of Akron, Akron, OH 44325, USA

ARTICLE INFO

Article history:
Received 24 July 2009
Received in revised form
13 November 2009
Accepted 18 January 2010

Keywords:
Titania
Alumina
Electrospinning
Sol–gel
Composite nanofibers

ABSTRACT

Composite fibers of TiO_2–Al_2O_3 were prepared by electrospinning a sol–gel and polymer mixture to form template polymeric fibers followed by calcination. The resulting fibers were characterized using thermogravimetric analysis (TGA), X-ray diffraction (XRD), diffuse reflectance ultraviolet–visible (UV–vis) spectroscopy, scanning electron microscopy (SEM), transmission electron microscopy (TEM), X-ray energy dispersive spectroscopy (XEDS), and X-ray photoelectron spectroscopy (XPS). Calcination at 973 K resulted in mixture of anatase (A) titania and gamma (γ) alumina phases. We calculated a band gap energy of 3.3 eV and found the average diameter of the resulting fibers in the 150–400 nm range. Both XEDS and XPS reveal that fibers are predominantly made of titania.

1. Introduction

Many technologically relevant processes occur on the surfaces of materials and material structures with greater surface-to-volume ratios are desired [1,2]. The performance of catalytic materials is directly related to the surface area and, hence, an increase in surface area of fibers as catalyst supports is expected to enhance their properties. The large surface area of these structures also makes them excellent materials for filtration applications [3]. Filtration properties of nanofibers can be further enhanced by growing carbon nanotubes on their surfaces [4]. In addition, nanofibers are considered for use as biomaterials in tissue engineering, mainly due to the interconnectivity of their 3-dimensional porous structures and large surface areas, similar to the morphology of a natural extracellular matrix [5]. They can also be used for gas sensors [6], where the large surface-to-volume ratio makes them ultrasensitive with fast response time.

Electrospinning provides a simple and direct method for manufacturing nanostructures [7]. In electrospinning a polymer precursor mixture, loaded in a syringe, is driven by a syringe pump to form a droplet at the tip of the needle. A high voltage (typically between 5 and 30 kV) is applied between the syringe needle and the collector. A jet launches from the droplet of the polymeric mixture when the electrical forces exceed those of surface tension and the jet elongates as it follows a spiraling path toward the collector. By controlling the experimental conditions one can influence the diameter of the resulting nanofibers, and their physical properties.

Alumina (Al_2O_3) [8,9] and titania (TiO_2) [10–15] nanofibers have previously been prepared using the sol–gel and electrospinning method whereas the composite alumina–titania nanofibers have recently been produced by a pH-swing preparation method with pH varying from 2 to 8 [16]. When a sol–gel method was used for synthesis of mixed alumina–titania structures it was found that the alumina–titania materials have a higher specific surface area than those of titania or alumina alone [17]. It is, therefore, of interest to further investigate these composite oxides especially since preparation of composite metal–oxide nanofibers has only been reported in a few studies. For instance, NiO/ZnO [18], TiO_2/SiO_2 [19], and Cr_2O_3/Al_2O_3 [20] composites have been prepared in this manner. Doping TiO_2 with Al has potential to improve photocatalytic activity of TiO_2 [21]. Even though the composite Al–Ti oxide nanofibers have recently been prepared via so-called

* Corresponding author.
E-mail address: gchase@uakron.edu (G.G. Chase).

0921-5107/$ – see front matter © 2010 Elsevier B.V. All rights reserved.
doi:10.1016/j.mseb.2010.01.027

pH-swing method combined with three different ways to incorporate titania precursor on alumina (co-precipitation, deposition, and stepwise deposition) with the calcinations temperature of 773 K [16], to the best of our knowledge, we present the first TiO_2–Al_2O_3 composite fibers prepared by mixing sol–gel precursor in a polymer mixture, electrospinning the mixture to form template polymer fibers, and calcinations of the template fibers to form the ceramic fibers. The advantage of our approach is that it is inexpensive and relatively simple. On the other hand, controlling the compositions of mixed oxides and the distribution of nanocrystals along the surfaces of the fibers for targeted applications remains one of the major challenges.

In this study, we synthesized composite titania–alumina fibers using the sol–gel and electrospinning method. The calcined fibers were characterized using thermogravimetric analysis (TGA), scanning electron microscopy (SEM), X-ray energy dispersive spectroscopy (XEDS), transmission electron microscopy (TEM), X-ray photoelectron spectroscopy (XPS), X-ray diffraction (XRD), and diffuse reflectance ultraviolet–visible (UV–vis) spectroscopy.

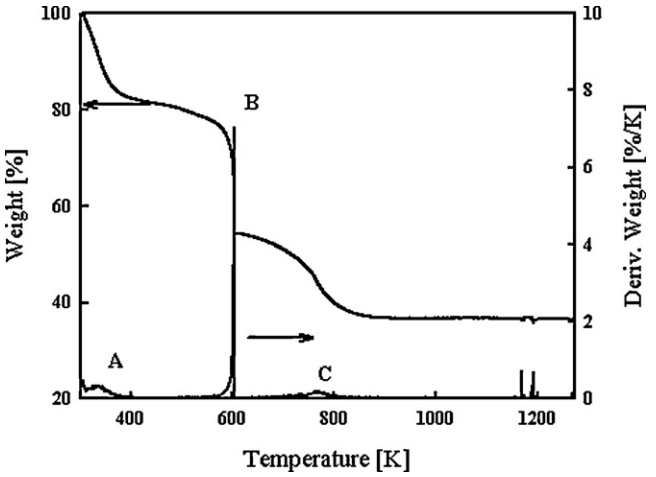

Fig. 1. TGA and first derivative curves of the as-spun fiber composite showing weight loss as a function of temperature, from room temperature to 1273 K. A heating rate of 10 K/min was used. The minor "bounce" in the curve that occurs at 1173 K is the result of disconnection of a N_2 gas line.

2. Experimental description

2.1. Synthesis of the fibers

The precursor polymer mixture for electrospinning was made by mixing aluminum acetate (Aldrich), methanol (Fisher Scientific), and glacial acetic acid (Fisher Scientific) at weight ratio of 1:15:1. The resulting solution was stirred continuously at 333 K for several hours to dissolve the ingredients. Tetraisopropyl titanate (Du Pont: Tyzor TPT Titanate) was added to the above solution at a weight ratio of 0.8:1 of tetraisopropyl titanate to the aluminum acetate–methanol–acetic acid solution and stirred until a clear homogeneous Ti–Al polymer mixture was achieved. A 2 g polymer solution of polyvinylpyrrolodone (PVP) in ethanol (PVP:ethanol = 1:13 wt ratio) was added to 1 g of the Ti–Al polymer mixture to obtain suitable mixture for electrospinning. The resulting mixture was transparent and yellow in color. The mixture was electrospun at a constant flow rate of 20 μl/min using a syringe pump, and was subjected to an applied voltage of 20 kV with a 15 cm gap distance between the tip and collector plates. The as-spun polymer fibers were calcined at 973 K to remove the organics and to form ceramic fibers.

Methanol is used as the solvent for the first solution described above because it yields a clear homogeneous solution. If ethanol is used as the solvent a white precipitate formed when mixed with the ethanol–PVP solution which did not electrospin well. Ethanol is preferred for the PVP solution because methanol evaporates too quickly and yields larger fibers. The PVP:ethanol ratio is important because it determines whether the mixture will electrospin, electrospray or not form a jet. For these materials the 1:13 wt ratio is in the range for electrospinning fibers.

2.2. Methods for characterization of the fibers

2.2.1. TGA

The formed fibers were analyzed using different techniques. TGA was perform using a Thermal Analyst 5000 with a Hi-Res TGA 2950 Thermogravimetric Analyzer, an air flow rate of 60 cc/min, and heating rate of 10 K/min.

2.2.2. XRD

A Phillips PW3710 X-ray Powder Diffractor with Copper Kα X-rays (λ = 0.154 nm) was employed for X-ray diffraction (XRD) analysis. The accelerating voltage was set to 45 kV and the current was kept at 40 mA. The step size was set to 0.020 (2θ, degrees) and the scan speed to 0.020 (2θ degrees per second).

2.2.3. UV–vis spectroscopy

UV–vis spectroscopy was done using a Cary 300 visible-UV spectrophotometer made by Varian. The scanning range was 12,500–50,000 cm^{-1} (1.5–6.2 eV) with a resolution of 16 cm^{-1}.

2.2.4. SEM and TEM

SEM images were acquired using Hitachi S-2150 at an accelerating voltage of 50 kV. Fiber sizes and morphology were also probed using a high-resolution transmission electron microscope (TEM, FEI Tecnai 12) by applying an accelerating voltage of 120 kV.

2.2.5. XEDS and XPS

The bulk elemental composition of the fibers was analyzed using X-ray energy dispersive spectroscopy (XEDS, FEI Quanta 200) operating at 25 kV whereas for surface elemental composition studies an X-ray photoelectron spectroscopy (XPS, VG ESCALAB MK II) system was used with an aluminum anode X-ray source operating at either 160 or 180 W power and typical operating pressure below 1×10^{-8} mbar. A pass-energy of 50 eV was used in the XPS experiments with a hemispherical analyzer.

3. Results and discussion

3.1. TGA of as-spun fibers

Fig. 1 shows the thermogravimetric analysis (TGA) results of as-spun polymer mixture fibers in the temperature range between room temperature and 1273 K. We observed the weight loss as a function of temperature: 21.5% loss between room temperature and 548 K, followed by 24.0% between 548 and 613 K, and finally 17.2% within the 613–873 K range. The weight loss is accompanied by a decrease in the diameter of the fibers as observed using an SEM (not shown). Above approximately 873 K there is no weight loss up to 1273 K and at these high temperatures one may expect the only material changes to be in the crystal structure. The total weight loss of our titania–alumina composite fibers of about 63% is similar to what was reported in a study of TiO_2 fibers [22]. The derivative weight loss curve, typically more sensitive to minute weight changes than the parent curve, merely confirms that the weight loss proceeds in three major steps. The first weight loss, below 373 K,

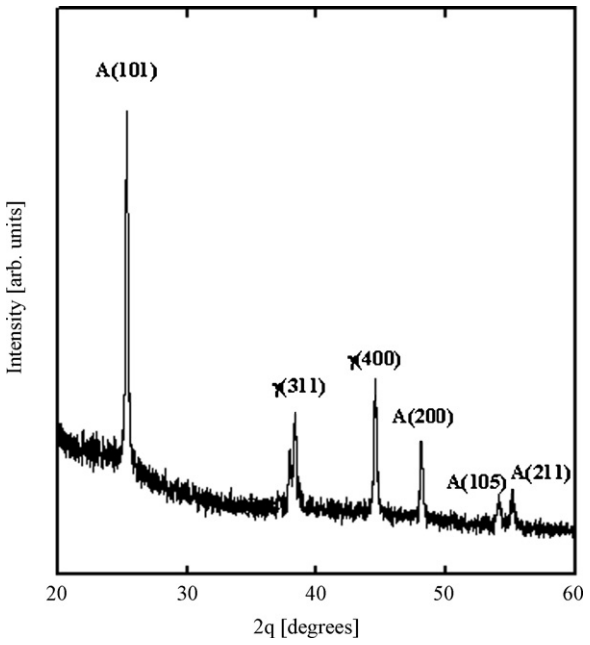

Fig. 2. The X-ray diffraction patterns of TiO_2–Al_2O_3 composite fibers calcined at 973 K. Major diffraction peaks are indicated as γ(*h k l*) phase of alumina and A(*h k l*) phase of titania, where A stands for anatase, and *h*, *k*, and *l* are Miller indices.

is likely due to loss of water vapor and trapped solvent, whereas peaks at about 623 and 773 K are likely due to loss of water crystals and degradation of the polymer, respectively, similar to what was reported by Nuansing et al. for TiO_2 fibers [23].

3.2. X-ray diffraction characterization of crystal phases

In the temperature range investigated above the TiO_2 can form three different phases: brookite, anatase, and rutile. The Ti atoms occupy sites within a deformed oxygen octahedral and the number of shared edges of the octahedra determines the crystal phase. Temperature plays an essential role in the formation of the crystal structures, and heating titania to 773 K typically results in the formation of only the anatase phase [24]. Heating the titania fibers to 873 K can result in a mixture of anatase and rutile phases and corresponds to the upper boundary of the exothermic reaction [15]. Our XRD results of titania–alumina composite fibers calcined at 973 K are shown in Fig. 2. The calcined fibers exhibit a mixture of anatase (A) titania and gamma (γ) alumina as indicated by the labels on the peaks in the figure.

The alumina γ(3 1 1) and γ(4 0 0) peaks and the anatase titania XRD features that our fibers exhibit after calcination at 973 K have previously been reported for alumina–titania nanofibers obtained via the pH-swing method following calcination at 773 K [16]. Even though the anatase-to-rutile phase transition of titania can occur at 873 K [15], our composite titania–alumina fibers show no evidence of the rutile titania phase at 973 K. It is possible that the presence of alumina within the fiber structure delays this phase transition.

3.3. Band gap energy evaluation

UV–vis diffuse reflectance data for the TiO_2–Al_2O_3 composite fibers calcined at 973 K are displayed in Fig. 3. Since our composite fibers are primarily composed of anatase titania at this calcination temperature and the anatase phase is known to have higher photocatalytic activity than rutile phase [25], it is relevant to determine the band gap energy value. The UV–vis data are presented as the Kubelka–Munk function spectrum, $F(R)$, that is related to

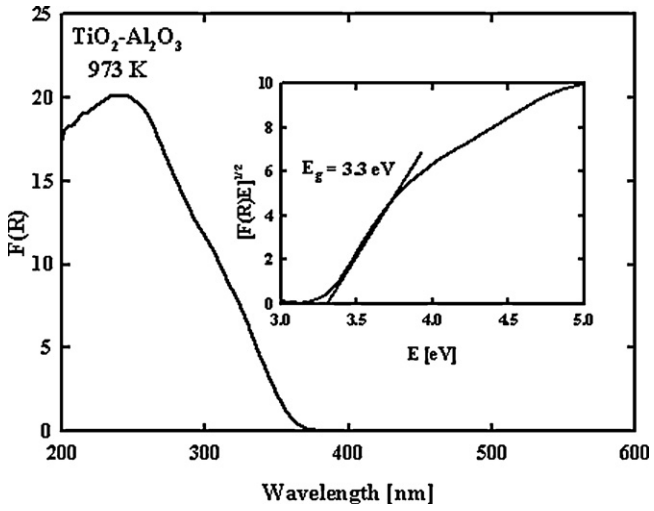

Fig. 3. The UV–vis diffuse reflectance of composite TiO_2–Al_2O_3 fibers annealed at 973 K presented as the Kubelka–Munk function, $F(R)$. The modified Kubelka–Munk function, $[F(R)E]^{1/2}$, versus photon energy, E, used for calculation of the energy band gap is shown in the inset.

the absorption coefficient, α, and scattering coefficient, s, via the formula:

$$F(R) = \frac{(1-R)^2}{2R} = \frac{\alpha}{s} \quad (1)$$

where R is reflectivity. Fig. 3 shows how these composite metal–oxide fibers absorb light as a function of photon energy. A plot of the modified Kubelka–Munk function, $[F(R)E]^{1/2}$, versus photon energy, E, is shown in the inset of Fig. 3, and is used to estimate the band gap energy E_g (the point of the intercept of the tangent line with the energy axis). We find $E_g = 3.3$ eV, which is in agreement with results reported for Al_2O_3–TiO_2 fibers (3.3–3.6 eV) [16] obtained via the pH-swing method and calcined at 773 K. Al–Ti oxide materials are being investigated for catalyst supports due to their textural and surface chemical properties, see Ref. [26] and references therein. Titania is a wide band gap oxide with $E_g > 3$ eV and is a promising material for photocatalysis applications [27]. On the other hand since doping TiO_2 with Al has potential to improve photocatalytic activity of TiO_2 [21], the calculation of the band gap energy is important in these applications.

3.4. Fiber morphology studies using SEM and TEM

The SEM and TEM images shown in Figs. 4 and 5, respectively, reveal the morphology of the resulting nonwoven fibers after calcination at 973 K. The diameters of the fibers following calcination are significantly smaller than the as-spun polymer fibers due to removal of organics, which is to be expected [10]. The fibers have large length-to-diameter ratios resulting in flexible mat structures with many pores for gases to flow through which is useful, for example, in thermophotovoltaics (TPV) applications [10]. The random orientations of the fibers are suitable in biomedical applications (tissue engineering scaffolds and wound dressing), for catalyst supports [28], and in filtration media [29]. The diameters of the majority of synthesized fibers range from 150 to 400 nm and the fibers appear to be composed of connected crystallites (Fig. 5).

3.5. XEDS and XPS elemental composition analysis

XEDS data acquired on the calcined fibers are displayed in Fig. 6. The spectra reveal signatures of oxygen, titanium, and aluminum, together with traces of carbon. The results in wt% (At%) reveal the following composition: 44% (69%) oxygen, 52% (27%) titanium, and

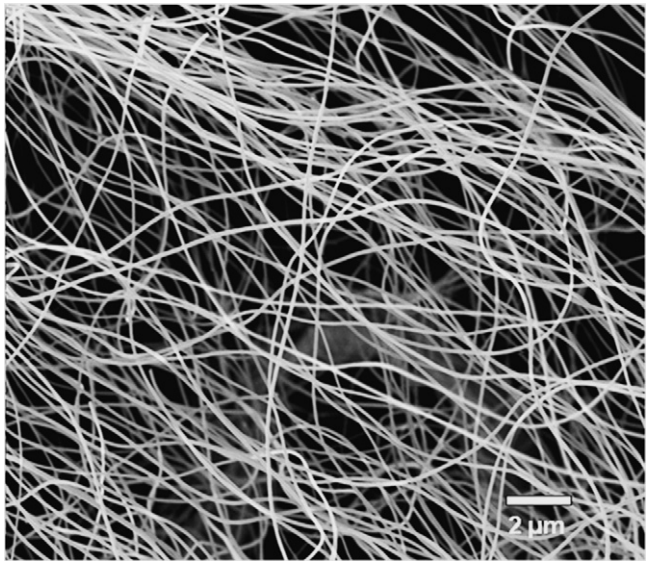

Fig. 4. Scanning electron micrograph of fibers calcined at 973 K.

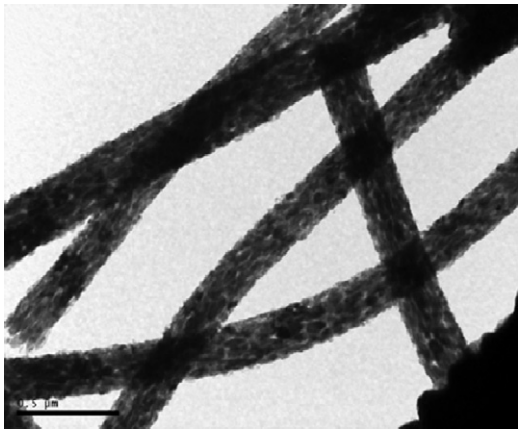

Fig. 5. TEM image of TiO_2–Al_2O_3 composite fibers calcined at 973 K. The scale bar is 500 nm.

4% (4%) aluminum. The Ti:Al ratio is the same (within experimental uncertainty) as the original polymer mixture prior to electrospinning. Carbon was not included in our percentage calculations since the tape used to support the fibers is a likely source of the carbon signal. We have recently tested this hypothesis of the origin of the XEDS carbon signal by increasing the quantity of fibers until the carbon signal disappeared (data not shown). XEDS data reveal that most of the structure of the fibers is composed of titania.

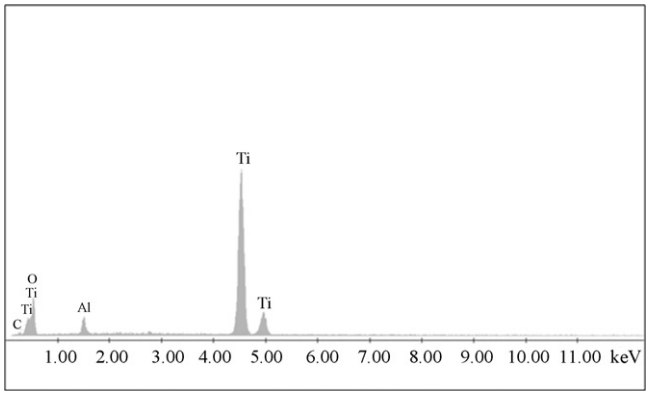

Fig. 6. X-ray energy dispersive spectroscopy (XEDS) of the calcined composite TiO_2–Al_2O_3 fibers.

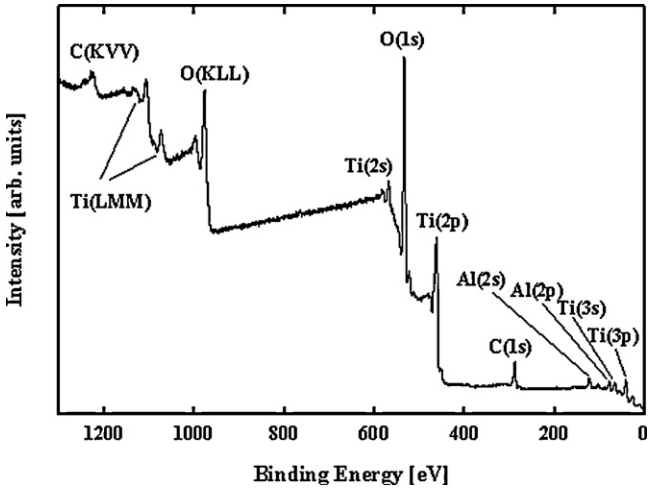

Fig. 7. X-ray photoelectron spectra of the TiO_2–Al_2O_3 composite fibers calcined at 973 K. C(KVV), Ti(LMM), and O(KLL) denote Auger electron signatures.

Information about the surface elemental composition of the fibers is obtained using XPS. Since many relevant processes such as adsorption or catalysis occur on surfaces, the presence of even trace amounts of impurities may have unwanted effects in the application of these fibers and, in that regard, XPS is a very powerful analytical method for our purposes [9]. Survey scans of composite alumina–titania fibers calcined at 973 K are presented in Fig. 7. XPS data clearly show signatures of O, Ti, and Al. A carbon signal is almost always seen in XPS as previously reported for calcined electrospun Al_2O_3 [9], TiO_2 [30], and Bi_2O_3 [31] fibers, and we cannot completely rule out surface contamination of the fibers from the process of handling and long exposures in air. However, part of carbon signal may as well originate from the supporting carbon-based tape, similar to what we determined in the XEDS experiments.

The elemental composition of the fibers does not change in the temperature range 873–1273 K, as can be inferred from TGA results which showed no change in weight after 873 K. The presence of both aluminum and titanium on the surface of the fibers is evident from the XPS spectra and demonstrates successful production of the composite metal–oxide fibers. The XPS spectral features were integrated and corrected for atomic sensitivity factors, yielding the following atomic percentages: Ti-18.3%, Al-13.5%, and O-68.2% with the carbon signal not included in the analysis. The fact that we observe more aluminum in XPS than in XEDS indicates that alumina predominantly resides on the surface of the fibers. The dispersion of alumina along the surface of titania nanofibers stabilizes the surface of the fibers and increases the activation energy for the nucleation of the rutile phase that starts at the surface, in agreement with our XRD results and with the literature [32]. These findings are relevant in catalysis applications of alumina–titania materials [33]. Our data indicate that for thorough characterization of the fibers, surface-sensitive methods such as XPS can play an important role [9]. The presence of forms of titanium dioxide other than TiO_2 has not been ruled out. Hence the end ratio between TiO_2 and Al_2O_3 in the composite fiber is uncertain. To avoid speculation only the elemental amounts of Ti, Al, and O are reported above.

Combining XEDS and XPS methods for the characterization of inhomogeneous samples is very powerful [34]. In the present case, both XEDS and XPS reveal that the fibers are primarily composed of titania. Since XPS is surface-sensitive in contrast to XEDS which is more of a bulk-sensitive method, the results complement one another.

4. Summary

The TiO_2–Al_2O_3 fibers were prepared by electrospinning of a polymer mixture containing the sol–gel precursors followed by calcination. The produced fibers were characterized using TGA, XRD, UV–vis, SEM, TEM, XEDS, and XPS. TGA results show there is no weight loss above 873 K. Hence, above this temperature the fibers only exhibit change in the crystalline structure. Fibers calcined at 973 K show both alumina (γ) and titania (anatase) phases. We determined the band gap energy to be 3.3 eV and found the diameters of the composite fibers to be in the range of 150–400 nm. The fibers are predominantly made of titania, with alumina favoring the surface of the fibers, as observed in XPS measurements. The combination of excellent physical and chemical properties of these fibers show they are excellent candidates for high-temperature applications, and in particular for photocatalytic applications since doping TiO_2 with Al has potential to improve the photocatalytic activity of TiO_2. Future studies will investigate how properties such as the band gap change with the fiber Ti–Al composition.

Acknowledgements

This work was supported by NSF grants IIP 0637539 and DMI-0403835. We thank R.H. Seiple for TGA measurements and S.V. Dordevic for use of his UV–vis system.

References

[1] G.M. Whitesides, Small 1 (2005) 172–179.
[2] C.A. Mirkin, Small 1 (2005) 14–16.
[3] X.-H. Qin, S.-Y. Wang, J. Appl. Polym. Sci. 102 (2006) 1285–1290.
[4] H. Hou, D.H. Reneker, Adv. Mater. 16 (2004) 69–73.
[5] J. Lannutti, D. Reneker, T. Ma, D. Tomasko, D. Farson, Mater. Sci. Eng. C 27 (2007) 504–509.
[6] S. Ji, Y. Li, M. Yang, Sens. Actuators B: Chem. 133 (2008) 644–649.
[7] C. Burger, B.S. Hsiao, B. Chu, Annu. Rev. Mater. Res. 36 (2006) 333–368.
[8] A.-M. Azad, Mater. Sci. Eng. A 435–436 (2006) 468–473.
[9] R.W. Tuttle, A. Chowdury, E.T. Bender, R.D. Ramsier, J.L. Rapp, M.P. Espe, Appl. Surf. Sci. 254 (2008) 4925–4929.
[10] V. Tomer, R. Teye-Mensah, J.C. Tokash, N. Stojilovic, W. Kataphinan, E.A. Evans, G.G. Chase, R.D. Ramsier, D.J. Smith, D.H. Reneker, Sol. Energy Mater. Sol. Cells 85 (2005) 477–488.
[11] R. Teye-Mensah, V. Tomer, W. Kataphinan, J.C. Tokash, N. Stojilovic, G.G. Chase, E.A. Evans, R.D. Ramsier, D.J. Smith, D.H. Reneker, J. Phys. Condens. Matter 16 (2004) 7557–7564.
[12] E.T. Bender, R. Wang, M.T. Aljarrah, E.A. Evans, R.D. Ramsier, J. Vac. Sci. Technol. A 25 (2007) 922–926.
[13] D. Li, J.T. McCann, M. Gratt, Y. Xia, Chem. Phys. Lett. 394 (2004) 387–391.
[14] R. Chandrasekar, L. Zhang, J.Y. Howe, N.E. Hedin, Y. Zhang, H. Fong, J. Mater. Sci. 44 (2009) 1198–1205.
[15] C. Tekmen, A. Suslu, U. Cocen, Mater. Lett. 62 (2008) 4470–4472.
[16] J.A. Munoz-Lopez, J.A. Toledo, J. Escobar, E. Lopez-Salinas, Catal. Today 133–135 (2008) 113–119.
[17] H.K. Farag, M. Al Zoubi, F. Endres, J. Mater. Sci. 44 (2009) 122–128.
[18] C. Shao, X. Yang, H. Guan, Y. Liu, J. Gong, Inorg. Chem. Commun. 7 (2004) 625–627.
[19] S. Zhan, D. Chen, X. Jiao, Y. Song, Chem. Commun. 20 (2007) 2043–2045.
[20] X. Yang, C. Shao, Y. Liu, J. Mater. Sci. 42 (2007) 8470–8472.
[21] J.E. Lee, S.M. Oh, D.W. Park, Thin Solid Films 457 (2004) 230–234.
[22] S.-H. Lee, C. Tekmen, W.M. Sigmund, Mater. Sci. Eng. A 398 (2005) 77–81.
[23] W. Nuansing, S. Ninmuang, W. Jarernboon, S. Maensiri, S. Seraphin, Mater. Sci. Eng. B 131 (2006) 147–155.
[24] D. Li, Y. Xia, Nano Lett. 3 (2003) 555–560.
[25] J. Augustinski, Electrochim. Acta 38 (1993) 43–46.
[26] J. Ramirez, G. Macias, L. Cedeno, A. Gutierrez-Alejandre, R. Cuevas, P. Castillo, Catal. Today 98 (2004) 19–30.
[27] A.L. Linsebigler, G. Lu, J.T. Yates Jr., Chem. Rev. 95 (1995) 735–758.
[28] E. Formo, M.S. Yavuz, E.P. Lee, L. Lane, Y. Xia, J. Mater. Chem. 19 (2009) 3878–3882.
[29] Y.J. Choi, M.J. Park, J.S. Hong, M.S. Hong, J.C. Lee, Korean J. Ceram. 5 (1999) 284–287.
[30] E.T. Bender, P. Katta, G.G. Chase, R.D. Ramsier, Surf. Interface Anal. 38 (2006) 1252–1256.
[31] C. Wang, C. Shao, L. Wang, L. Zhang, X. Li, Y. Liu, J. Colloid Interface Sci. 333 (2009) 242–248.
[32] X. Ding, L. Liu, X. Ma, Z. Qi, Y. He, J. Mater. Sci. Lett. 13 (1994) 462–464.
[33] K. Kawabata, H. Yoshimatsu, K. Fujiwara, T. Yabuki, A. Osaka, Y. Miura, J. Mater. Sci. 34 (1999) 2529–2534.
[34] N. Stojilovic, J.D. Ehrman, E.T. Bender, J.C. Tokash, R.D. Ramsier, M.W. Kovacik, Appl. Surf. Sci. 252 (2006) 3760–3766.